Catalysis Today 175 (2011) 346–355

Contents lists available at ScienceDirect

Catalysis Today

journal homepage: www.elsevier.com/locate/cattod

Preparation and catalytic activity of Fe alginate gel beads for oxidative degradation of azo dyes under visible light irradiation

Yongchun Dong*, Wenjing Dong, Yanan Cao, Zhenbang Han, Zhizhong Ding

Division of Textile Chemistry and Ecology, School of Textiles, Tianjin Polytechnic University, 63 Chenglin Road, Hedong District, Tianjin 300160, China

ARTICLE INFO

Article history:
Received 14 October 2010
Received in revised form 20 February 2011
Accepted 14 March 2011
Available online 9 April 2011

Keywords:
Ferric ion
Alginate
Gel bead
Fenton catalyst
Dye degradation

ABSTRACT

Fe alginate gel beads were prepared by adding sodium alginate aqueous solution drop-wise into the $FeCl_3$ gelling solution using a syringe needle at room temperature, and measured in terms of size, mass and Fe content, then characterized using SEM, XRD, FT-IR, XPS and TGA, respectively. The gel beads were evaluated as the heterogeneous Fenton catalysts for oxidative degradation of two typical azo dyes, Reactive Blue 222 and Acid Black 234 in the presence of H_2O_2 under visible light irradiation. Some important factors affecting the preparation of the beads and their catalytic function such as $FeCl_3$ concentration, irradiation intensity and pH value were examined. The results indicated that Fe^{3+} ions coordinated with oxygen atoms in carboxyl groups from glucose chains of alginates to form the Fe alginate gel beads. And Fe^{3+} ion was a central cation that has a coordination number of 6 in the complex. Higher concentration of $FeCl_3$ solution caused the significant increase in the Fe content of the gel bead during preparation. Fe alginate gel beads showed a great catalytic role in the degradation of the azo dyes in a wide pH range of 3.0–8.0. Moreover, higher Fe content and increasing irradiation intensity could promote the catalytic performance of Fe alginate gel beads.

1. Introduction

Photoassisted Fenton technologies have been widely used in the degradation of water-soluble organic dyes in the industrial wastewater. Ferrous salts react with H_2O_2 to produce hydroxyl free radicals during the Fenton reaction, which attack the unsaturated dye molecules, thus decolorizing the wastewater [1]. However, it should be noticed that Fenton reactions are limited to the acidic $pH < 4$. Moreover, the Fe ion sludge with a large volume after Fenton reaction is a considerable drawback because the removal of the Fe ions at the end of treatment by precipitation is rather a costly process. To avoid these limitations, some attempts have been made to develop the heterogeneous photocatalysts for the Fenton reactions by immobilizing Fe ions on the polymer substrates. For example, a Nafion membrane [2–4] or pellet [5] was used for immobilizing Fe ions to form a Fe/Nafion catalyst for the decoloration of azo dye in water. But, it is known that Nafion membrane or pellet is too expensive to be used as a catalyst support in an industrial scale [6]. Hence, it is necessary to explore new heterogeneous catalysts for the photoassisted Fenton reactions by using lower cost polymer materials as the support substrates. The fibrous heterogeneous Fenton catalysts were produced by ligating reaction between modified polyacrylonitrile fibers and ferric ions. And it was found that the dyeing wastewater was decolorizied with H_2O_2 in the presence of fibrous catalysts [7,8].

Alginate acid is a naturally occurring linear polysaccharide composed of (1–4)-linked-D-mannuronic acid (M units) and -L-guluronic acid (G units) monomers, which vary in amount and sequential distribution along the polymer chain depending on the source of the alginate [9]. Moreover, because of the unique gelling properties, alginates can react with metal ions to form stable organic–inorganic hybrid composite materials, which may be found promising applications in the environmental purification and remedy areas [10–13]. In addition, it has been reported that complex of Fe ions with alginate was active during the Fenton-enhanced degradation of Orange II [12]. However, the information regarding preparation and catalytic function of Fe alginate gel beads as the heterogeneous Fenton catalysts for the degradation of the organic pollutants is still scarce. In the present study, we aim to prepare and characterize the Fe alginate gel beads and evaluate their catalytic property in the oxidative degradation of two azo dyes in the presence of H_2O_2. The influence of some important variables on the preparation and catalytic performance of the beads was also investigated. In addition, we are more concerned about whether Fe alginate gel beads have better catalytic performance for the dye degradation at or over pH 5.0 to avoid the costly initial pH adjustment of many effluents to attain acidic conditions before applying the oxidative treatment.

---

* Corresponding author. Tel.: +86 22 24528430; fax: +86 22 24528054.
E-mail addresses: dye@tjpu.edu.cn, dyefib@yahoo.com.cn (Y. Dong).

0920-5861/$ – see front matter © 2011 Elsevier B.V. All rights reserved.
doi:10.1016/j.cattod.2011.03.035

2. Experimental

2.1. Materials and reagents

Sodium alginate and $FeCl_3 \cdot 7H_2O$ were of agent grade and obtained from Shanghai Medical Co. (Shanghai, China). Two azo dyes including Reactive Blue 222 (Abbr. RB 222) and Acid Black 234 (Abbr. AB 234) were commercially available, and purified by reprecipitation method in this experiment, the molecular structures of which are presented in Scheme 1. Double distilled and deionized water was used throughout the study.

2.2. Preparation of Fe alginate gel beads

A given concentration of sodium alginate aqueous solution was prepared by dissolving the appropriate weight of solid sodium alginate in distilled water. Five milliliters of sodium alginate solution was added drop-wise into a 250 ml $FeCl_3$ gelling solution using a 1.0-mm syringe needle at a dropping rate of approximate 1.0 ml min^{-1} at room temperature to produce the Fe alginate gel beads. These brown beads were cured for 6 h in the gelling solution with mild stirring (60 rpm) using magnetic mixer at room temperature, and then filtered off and washed repeatedly with distilled water, and stored in distilled water for the dye degradation study.

2.3. Determination of coordination number for Fe alginate complex

To determine the coordination number for Fe alginate complex, an electric conductivity method reported by Cheng et al. [14] was used in this work. Different concentrations (0.25–12.0 mmol L^{-1}) of $FeCl_3$ aqueous solution were prepared and mixed with 3.00 mmol L^{-1} sodium alginate aqueous solution at the same volume (25 ml) in order to obtain a series of reaction systems with different molar ratios of the concentration of $FeCl_3$ to the concentration of sodium alginate in solution. The coordination reactions in these systems were conducted at 25 °C until the reaction equilibrium was reached. And the electric conductivities for different concentrations of $FeCl_3$ solutions before and after coordination reaction were determined using a DDSJ-308A conductivity meter (Shanghai Jingmi Instrumental Co., China). Then the difference in the electric conductivity between $FeCl_3$ solutions before and after coordination reaction for each concentration was calculated and used to determine the coordination number for the resulting complex of Fe^{3+} ion with alginate. It is noticed that the electric conductivities of distilled water and 3.00 mmol L^{-1} sodium alginate aqueous solution were also measured to be 1.12×10^{-2} ms cm^{-1} and 1.29 ms cm^{-1} at 25 °C, and took out from the calculation for the electric conductivities of $FeCl_3$ solutions and reaction systems, respectively.

2.4. Characterization for Fe alginate gel beads

2.4.1. Diameter and mass

The diameter and mass of Fe alginate gel beads in wet or dry state were measured using digital vernier calipers and balance, respectively, and then mean diameter and mean mass of each gel bead were obtained by the measurement of 20 beads out of approximately 200.

2.4.2. Fe content ($C_{Fe\text{-}bead}$)

In order to determine the Fe content immobilized on the surface of Fe alginate gel beads, they were selected randomly and treated with 50 ml of 2.0 mol L^{-1} H_2SO_4 aqueous solution at room temperature for 24 h. Fe^{3+} ions were released from Fe alginate gel beads and dissolved in acidic solution. And then the concentration of Fe^{3+} ions in the solution was determined by using a WXF120 atomic absorption spectrometer (Beijing Rayleigh Analytical Instrument Co.), for calculating total Fe content of the beads. Average Fe content for single bead was obtained by the measurement of 20 beads out of approximately 200.

2.4.3. Composition and structure

The composition of Fe alginate gel bead was verified by using a Nicolet Magna-560 Fourier transform spectrometer (Nicolet Instrument Co., USA) with 4 cm^{-1} resolution. The powder X-ray diffraction measurement of the bead was conducted on a Rigaku Xd/Max-2500 X-ray diffractometer (Rigaku Co., Japan) operating with Cu Ka radiation at 40 kV and 20 mA, 2θ ranges from 5° to 80°, and the scan rate used was 0.025°/min. The binding energy analyses were performed on a PHI 5600 X-ray photoelectron spectrometer (Pekin Elmer Co., USA), and binding energy of C1s was shifted to 284.8 eV as the reference. The surface morphology of Fe alginate gel beads was examined by FEI Quanta 200 scanning electron microscope (FEI Co., USA). TGA (Thermal Gravimetrical Analysis) of the samples was carried out with a STA 409 PC thermal analyzer (NETZSCH Co., Germany). TGA of the samples was performed up to a temperature of 700 °C, with a starting point at room temperature in an atmosphere of nitrogen. The heating rate was uniform in all cases at 10 °C min^{-1}.

2.5. Activity towards H_2O_2 decomposition

100 Fe alginate gel beads as the catalysts were placed into the reactor containing 150 ml of 0.10 mol L^{-1} H_2O_2 aqueous solution. Air was delivered to the H_2O_2 solution from the bottom of the reactor in order to ensure thorough mixing of the beads with the solution. The reaction temperature was 25 °C, and air supply was 100 ml min^{-1}. To examine the H_2O_2 decomposition in the presence of the beads, 1–2 ml of samples were withdrawn for analysis of the residual H_2O_2 concentration at intervals of time and analyzed by titration with 0.02 mol L^{-1} concentration of $KMnO_4$ solution [7]. The analysis of the residual concentration of H_2O_2 was repeated three times for each sample and the results were averaged.

2.6. Photocatalytic reaction setup

The photoreaction system was specially designed in this experiment and consisted mainly of chamber, lamp, electromagnetic valve, relay, and water bath. A 400 W high pressure mercury lamp (Foshan Osram Illumination Co., China) was used as illuminating source for photocatalytic reaction. A cut-off filter was used to ensure irradiation only by visible light ($\lambda > 420$ nm). The chamber was made of polished aluminum because it is highly reflective in the visible light range. Ten open Pyrex vessels of 150 ml capacity were used as reaction receivers in water bath. An electromagnetic valve was operated by relay and used to control temperature in water bath. The intensity of visible light irradiation over the surface of test solution was controlled by adjusting the distance between lamp and surface of test solution, and was measured using FZ-A radiometer (Beijing BNU Light and Electronic Instrumental Co., China). The schematic diagram of photoreaction system was described in Fig. 1.

2.7. Photocatalytic procedure and analysis

Stock dye solutions were prepared by dissolving 5.0 g of each dye in 1000 ml of boiling deionized water. Test solutions (100 ml) were made by diluting the stock to typical effluent dye concentration of 0.05 mmol L^{-1} and followed by addition of 3.0 mmol L^{-1} H_2O_2 and 50 Fe alginate gel beads (unless otherwise stated). And NaOH (0.10 mol L^{-1}) and HNO_3 (0.10 mol L^{-1}) solutions were used to adjust pH values. Test solutions were then placed into reaction

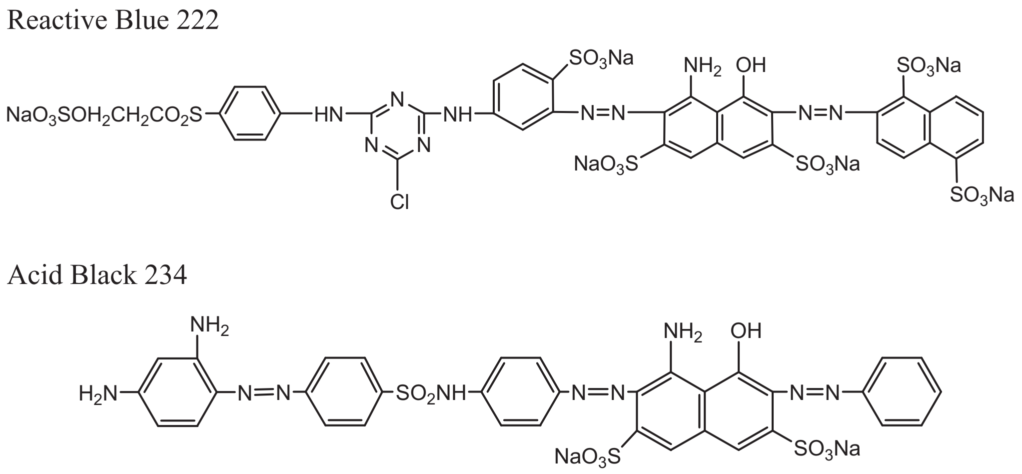

Scheme 1. Chemical structures of two azo dyes.

vessels and exposed to the irradiation of lamps in photoreaction system. At different time intervals, 1–2 ml of the test solution was withdrawn and diluted suitably, and the absorbance of which was measured at the λ_{max} (610 nm for RB 222 and 452 nm for AB 234) of the dye solution. The pH of the solution was measured using DHS-25C digital pH meter (Shanghai Jingmi Instrumental Co., China). The temperature in reaction vessel was kept at $25 \pm 1\,^{\circ}C$. The decoloration percentage of the dye was expressed as: $D\% = (1 - C/C_0) \times 100$, where C_0 is the initial concentration of the dye ($mmol\,L^{-1}$) and C is the residual concentration of the dye ($mmol\,L^{-1}$). TOC was measured with a Phoenix 8000 TOC analyzer (Tekmar-Dehrmann Crop., USA) and the TOC removal percentage of the dye was calculated as follows: TOC removal $\% = (1 - TOC_t/TOC_0) \times 100$, where TOC_0 is the initial TOC value of the dye solution ($mg\,L^{-1}$) and TOC_t is the residual TOC value of the dye solution ($mg\,L^{-1}$). ESR (electron spin resonance) signals of the hydroxyl radical spin-trapped by DMPO (5,5-dimethyl-1-pyrroline N-oxide) were examined on a Bruker ESP 300E spectrometer with an irradiation source of Quanta-Ray Nd:YAG pulsed laser system ($\lambda = 532$ nm).

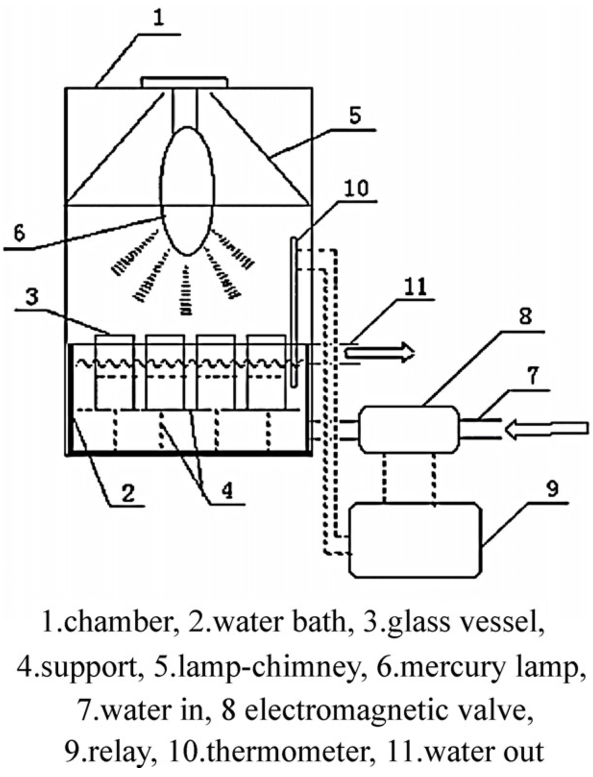

Fig. 1. The schematic diagram of photoreaction system.

3. Results and discussion

3.1. Preparation of Fe alginate gel beads

Generally, Fe alginate gel beads were produced by the reaction of sodium alginate with Fe^{3+} ions in the aqueous solution, and their mass, diameter and Fe content were affected significantly by the concentration of sodium alginate or $FeCl_3$ solution. To determine the dependence of the mass, diameter and Fe content of the beads on sodium alginate concentration during the preparation, the varied concentrations (2.0–4.0 wt%) of sodium alginate aqueous solutions were dropped into $0.10\,mol\,L^{-1}$ $FeCl_3$ aqueous solutions, respectively to prepare different size of Fe alginate gel beads, and the result was presented in Table 1.

Table 1 shows that increasing concentration of sodium alginate solution is accompanied by increasing mass, diameter and Fe content of the beads in the wet or dry state. This indicated that increasing the number of alginate acid chains could react with much Fe^{3+} ions in solution to form large size of gel beads with high Fe content because alginate acid has a unique property of gel-formation in the presence of multivalent metal ions in aqueous media [15,16]. On the other hand, in order to investigate the effect of $FeCl_3$ concentration, Fe alginate gel beads were prepared by the gelation of 3.0 wt% concentration of sodium alginate solution in different concentrations of $FeCl_3$ solutions. The mass, size and Fe content of the obtained beads were listed in Table 2.

As shown by the data in Table 2 that the mass and diameter of the beads varied insignificantly with $FeCl_3$ concentration, thus suggesting that the size of the beads could hardly be affected by $FeCl_3$

Table 1
Effect of sodium alginate concentration (C_{SA}) on mass, diameter and Fe content of Fe alginate gel bead.

C_{SA} (wt%)	M_w (mg)	M_d (mg)	D_w (mm)	D_d (mm)	$C_{Fe\text{-}bead}$ (mg)
2.0	29.77	1.10	4.07	1.39	0.415
3.0	33.20	2.09	4.23	1.46	0.487
4.0	39.12	4.23	4.41	1.51	0.647

M_w or M_d: mean mass of single wet or dry bead and D_w or D_d: mean diameter of single wet or dry bead.

Table 2
Effect of $FeCl_3$ concentration (C_{FeCl_3}) on mass, diameter and Fe content of Fe alginate gel bead.

C_{FeCl_3} (mol L^{-1})	M_w (mg)	M_d (mg)	D_w (mm)	D_d (mm)	$C_{Fe\text{-}bead}$ (mg)
0.05	28.2	2.09	4.23	1.58	0.372
0.10	30.2	2.11	4.14	1.65	0.415
0.15	33.2	2.16	4.15	1.62	0.726
0.20	33.5	2.17	3.99	1.63	0.872

concentration. However, it should be noticed that Fe content of the gel bead increases remarkably as $FeCl_3$ concentration increases. This demonstrates that increasing the $FeCl_3$ concentration is crucial for obtaining high Fe content of the gel beads. Moreover, when $FeCl_3$ concentration increases to 0.20 mol L^{-1}, Fe content of the obtained gel bead is 0.872 mg, which is higher than that of Fe-doped Ca-alginate gel bead reported in previous studies [13,17].

On the basis of above experimental results and literature information, the conditions for the Fe alginate gel bead with optimal Fe content (0.70–0.85 mg) were proposed to be $C_{SA} = 3.0$ wt% and $C_{FeCl_3} = 0.10$ mol L^{-1}. This is similar to the conditions used in the literature [12]. Since sodium alginate solution with higher than 3.0 wt% may show too high viscosity to be used for the preparation of Fe alginate gel beads with uniform size by using a 1.0-mm syringe needle. Besides, although higher concentration of $FeCl_3$ solution can increase Fe content of the resulting gel beads, the usage of $FeCl_3$ solution with the excessively high concentration is not available commercially at a low-cost. Moreover, to determine the coordination number of Fe^{3+} ions with alginate for the gel beads with optimal Fe content, the electrical conductivities of different concentrations of $FeCl_3$ solutions before and after coordination reaction in reaction systems were measured and summarized in Table 3.

The data in Table 3 indicate that k_1 and k_2 values increase gradually with C_{FeCl_3} increasing. And the difference (k_d) between k_1 and k_2 shows the similar increase tendency at low C_{FeCl_3}, but little change is observed when C_{FeCl_3} is higher than 1.00 mmol L^{-1}. This is because the coordination of sodium alginate with Fe^{3+} ions leads to a decrease in the quantity of free Fe^{3+} ions in solution. And a saturated coordination between them is obtained at $C_{FeCl_3} = 1.00$ mmol L^{-1}. A corresponding critical molar ratio C_{FeCl_3}/C_{SA} is found to be 1:3 from Table 3. Thus, it is believed that Fe^{3+} ion as a central cation has a coordination number of 6 in Fe alginate complex.

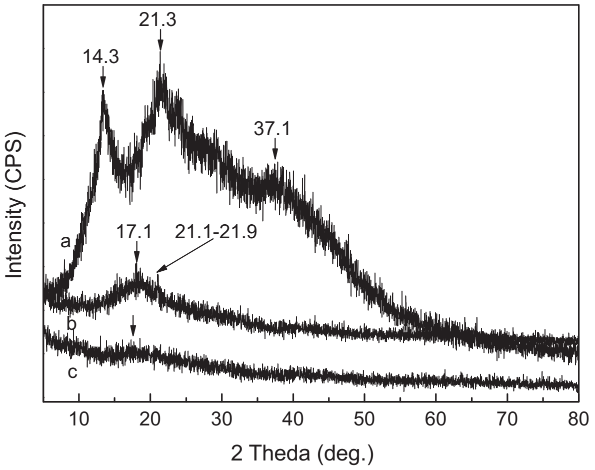

Fig. 3. XRD spectra of (a) sodium alginate, (b) Fe alginate gel bead prepared with 0.10 mol L^{-1} and (c) 0.20 mol L^{-1} $FeCl_3$ solution.

3.2. Characterization of Fe alginate gel beads

3.2.1. Morphology observation

The typical surface morphology of the dry spherical bead prepared with 3.0 wt% sodium alginate and 0.10 mol L^{-1} concentration of $FeCl_3$ is shown in Fig. 2.

Fig. 2 reveals that the surface of the gel bead is regular undulating, especially with some scattered wrinkles. This may be explained by so-called "egg-box" structure because guluronate blocks from sodium alginate molecule chains are responsible for the "egg-box" formation with Fe^{3+} ions during alginate gelation. Moreover, the biopolymer carrying carboxylic group is capable of forming complexes with metal ions at sufficiently high concentrations and some metal cations can cooperatively bind between the G-blocks of adjacent alginate chains [18]. Therefore, it can be suggested that the Fe species preferentially located at the surface of the bead are Fe^{3+} ions because the surface complex formation involving Fe carboxylate seems to be the mechanism for trivalent metal ion cross-linking of the alginate network [12].

3.2.2. XRD analysis

The X-ray diffraction curve of Fe alginate gel bead is presented in Fig. 3. As shown in Fig. 3, sodium alginate has three typical characteristic peaks (14.3°, 21.3° and 37.1°), which were similar to those published in the literature [19,20]. It is noticed that these peaks

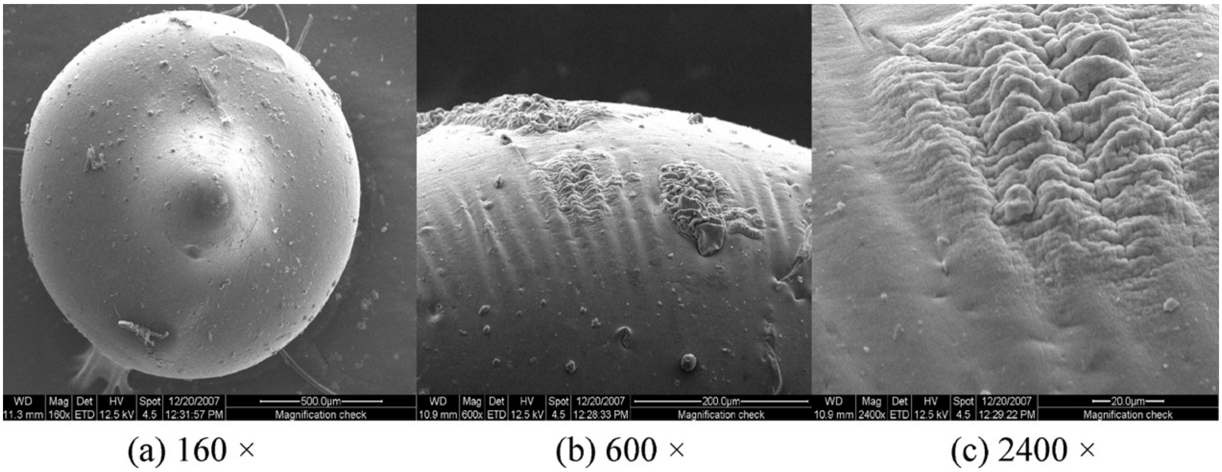

(a) 160 × (b) 600 × (c) 2400 ×

Fig. 2. SEM images of the dry Fe alginate gel bead.

Table 3
The electric conductivities of $FeCl_3$ and sodium alginate–$FeCl_3$ solution in different reaction systems.

Samples	$FeCl_3$ solution		Sodium alginate–$FeCl_3$ solution			
	C_{FeCl_3} (mmol L^{-1})	k_1 (ms cm^{-1})	C_{SA} (mmol L^{-1})	C_{FeCl_3}/C_{SA}	k_2 (ms cm^{-1})	$k_d = k_1 - k_2$
1	0.25	1.65	3.00	1:12	0.69	0.96
2	0.50	3.21	3.00	1:6	1.94	1.27
3	0.75	3.65	3.00	1:4	2.07	1.58
4	1.00	4.08	3.00	1:3	2.21	1.87
5	1.25	5.12	3.00	1:2.4	3.23	1.89
6	1.50	5.98	3.00	1:2	4.07	1.91
7	3.00	9.86	3.00	1:1	7.93	1.93
8	6.00	17.86	3.00	1:0.5	15.92	1.94
9	9.00	25.47	3.00	1:0.33	23.52	1.95
10	12.0	31.23	3.00	1:0.25	29.28	1.95

k_1 and k_2 are the electric conductivities of $FeCl_3$ solutions before and after adding sodium alginate solution, respectively.

almost disappeared as the complex was formed between alginate and Fe^{3+} ion, especially with higher concentration. More importantly, two new peaks at 17.1° and 21.1–21.9° are observed for Fe alginate gel beads, which may be due to the coordination of Fe^{3+} ions with the carboxyl groups of alginate molecule.

3.2.3. FT-IR analysis

Fig. 4 shows that a broad peak at 3450 cm^{-1} (V) in the spectrum of sodium alginate is attributed to the hydroxyl groups, and little change in its peak position and intensity was observed after the reaction of alginate molecule with Fe^{3+} ions. Consequently, this cannot be taken as evidence for the coordination of the oxygen atom in hydroxyl groups with Fe^{3+} ions when preparing the beads. The band at 2930 cm^{-1} (IV) is assigned to the stretch vibration absorption of C–H from glucose units in alginate chains [21]. The corresponding band becomes very weak in the spectrum of Fe alginate gel bead. This is because the egg-box structure limits the stretch vibration of C–H during the formation of the bead. Moreover, two bands at 1610–1620 cm^{-1} (III) and 1410 cm^{-1} (II) are assigned to the asymmetric and symmetric stretching vibrations of the carboxyl group (C–O–O) of alginate molecule, respectively [15,22]. It is obvious that both of them shifted to 1580–1590 cm^{-1} and 1430–1440 cm^{-1} in the spectra of Fe alginate gel bead. It should be pointed out that for Fe alginate gel bead, the antisymmetric band shifts to lower wavenumbers and the symmetric band towards higher wavenumbers compared to the sodium alginate bands. A similar band shift trend was also reported when some bivalent metal ions (Ca^{2+}, Zn^{2+}, Ni^{2+} and Cd^{2+}) coordinated with alginate [15]. But the shift extents (6.3–19.7 cm^{-1} for antisymmetric band and 4–6.9 cm^{-1} for symmetric band) for four bivalent metal alginate complexes in the literature [15] are much lower than those (30 cm^{-1} for antisymmetric band and 20–30 cm^{-1} for symmetric band) for Fe alginate gel bead in this work. Moreover, a new peak at 1700–1710 cm^{-1} (VI) in the spectrum of Fe alginate gel bead may also belong to the absorption vibrations of the carboxyl group of alginate molecule. The big difference in these carboxyl group bands of Fe alginate gel bead from the bivalent metal alginate complexes may be attributed to the higher coordination ability of Fe^{3+} ions with alginate, which is considered as a result of the stronger polarity of Fe^{3+} ions [7] and lower ligand field stabilization energy (LFSE) of Fe^{3+} complexes [23]. These results indicate a surface gelation of sodium alginate can be formed by the complex of their carboxyl groups with Fe^{3+} ions in aqueous solution. Additional sharp peak at 1060–1090 cm^{-1} (I) is for the C–O groups [24], but a significant change in its shape and position is not found in the gel beads.

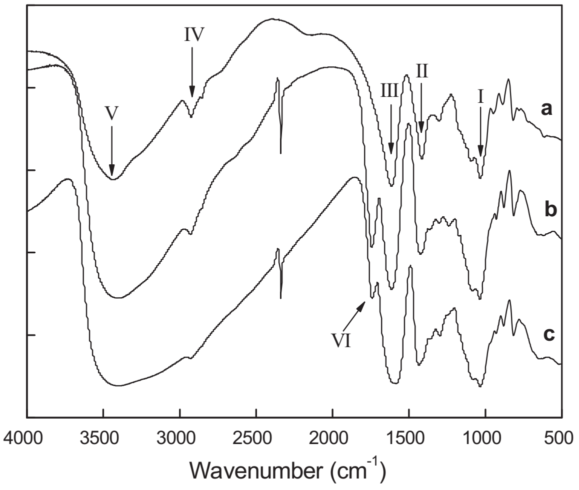

Fig. 4. FT-IR spectra of (a) sodium alginate, (b) Fe alginate gel bead prepared with 0.10 mol L^{-1} and (c) 0.20 mol L^{-1} $FeCl_3$ solution.

3.2.4. XPS analysis

The XPS survey spectrum and quantitative surface chemical composition of Fe alginate gel bead were determined, and the results are shown in Fig. 5, Tables 4 and 5.

As can be seen from Fig. 5 and Table 4, the main elements detected from the surface of Fe alginate gel bead included C, O and Fe; and no Na was detected. This result confirmed the opinion of Fernandez et al. [12] that alginate chains were bound by the Fe^{3+} ions and that the Fe^{3+} ions replaced the Na^+ ions on the surface of the bead. Consequently, we believed that the Fe^{3+} ions in aque-

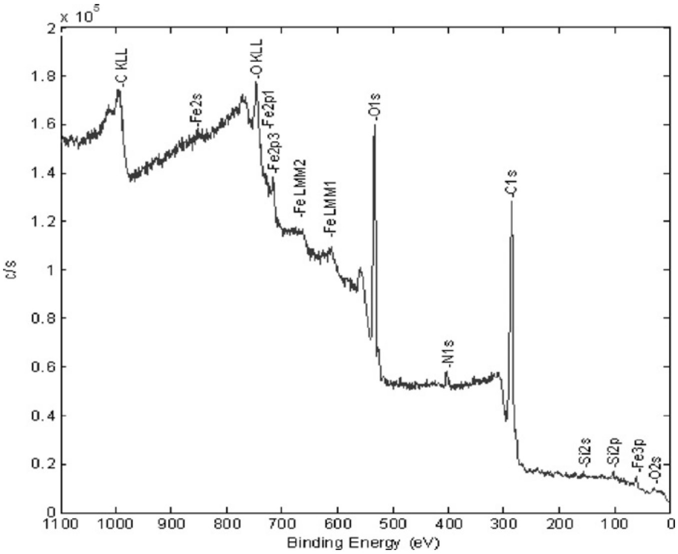

Fig. 5. XPS survey spectrum of Fe alginate gel bead.

Table 4
Surface chemical compositions (at.%) of Fe alginate gel bead determined by XPS.

Elements	C1s	O1s	Fe2p	Na1s	N1s	Si2p	Cl2p
Fe alginate gel bead	72.9	22.1	1.9	0.0	1.6	1.5	0.0
Sodium alginate	72.9	23.6	0.0	2.6	0.0	0.0	0.9

Table 5
Binding energy of sodium alginate, $FeCl_3$ and Fe alginate gel bead.

XPS peaks	Sodium alginate	$FeCl_3$	Fe alginate gel bead
C1s	284.6	–	284.7
O1s	532.4	–	534.0
Fe2p	–	711.3	710.8

ous solution could significantly exchange with the Na^+ ions of the functional carboxylic groups of the alginate strands when preparing the beads. Moreover, Fig. 5 and Table 5 show that the binding energy of the Fe2p in Fe alginate gel bead is 710.8 eV, lower than that (711.3 eV) of the Fe2p in $FeCl_3$, indicating that Fe^{3+} ions coordinated with carboxyl groups of glucose chain to form Fe alginate complexes. On the other hand, the binding energy of the O1s in the Fe alginate gel bead shifts to higher binding energy level. This means that oxygen atom in carboxyl group from alginate molecule as the electron donor can coordinate with the Fe^{3+} ion to form Fe alginate gel bead. This is consistent with the result obtained by FTIR method. Accordingly, it is fact that Fe^{3+} ions have been incorporated to alginate molecule when forming the bead. Besides, the result also reveals that the Fe detected is mainly Fe^{3+}, thus, indicating that the active sites on the surface of the beads could be Fe containing points.

3.2.5. TGA analysis

As can be seen from Fig. 6, the thermograms for both the samples showed similar trends. With increasing temperature the weight of sodium alginate decreased slowly up to 220 °C, and rapidly in the 220–280 °C range, then slowly again at higher temperature. The initial weight loss of sodium alginate may be caused by the presence of water in the sample and its lactonization. In 220–280 °C region, the percent weight loss was caused by breaking of sodium alginate backbone into the stable intermediates and loss of abundant hydroxyl groups on the sodium alginate in the form of water [24]. At higher temperature, sodium alginate would decarboxylate to form CO_2. Sodium alginate was not completely degraded in 500–700 °C. It maintained a weight percent of over 30% in this temperature range, which is similar to the result reported by Tripathy and Singh [24]. However, it should be noticed that that the weight loss of Fe alginate gel bead is lower than that of sodium alginate when temperature is within about 350 °C, indicating that Fe alginate gel bead has a greater heat stability compared with sodium alginate in this temperature range. These results imply that the Fe^{3+} ions may crosslink with the carboxyl groups in alginate chains to form the Fe alginate complexes during the reaction.

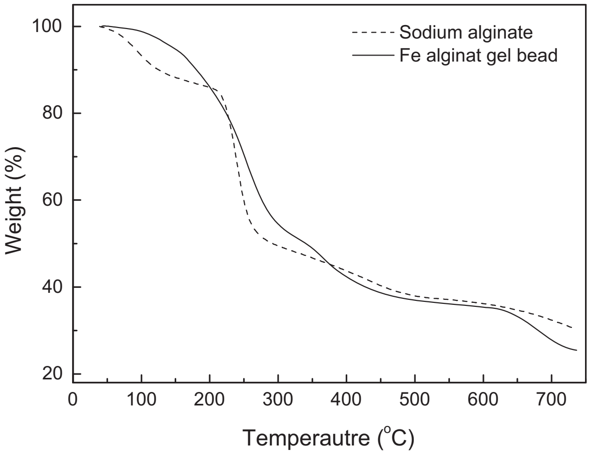

Fig. 6. TGA curves of sodium alginate and Fe alginate gel bead prepared with 0.20 mol L^{-1} $FeCl_3$ solution.

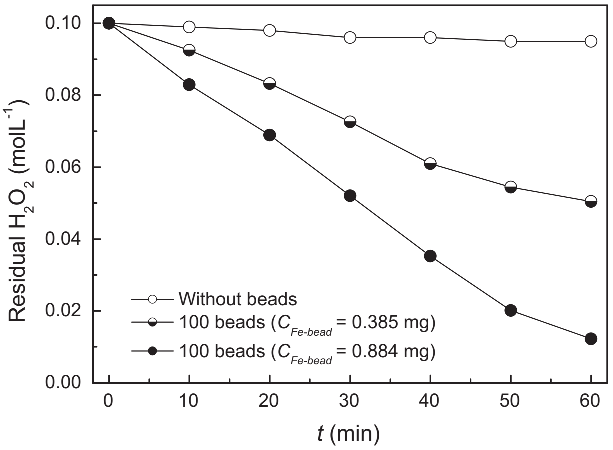

Fig. 7. Effect of Fe content of Fe alginate gel bead on H_2O_2 decomposition.

3.2.6. Activity towards H_2O_2 decomposition

The catalytic activity of Fe alginate gel bead was determined with respect to the decomposition of H_2O_2 and the results are presented in Fig. 7.

The decomposition of H_2O_2 under visible irradiation is not observed in the absence of Fe alginate gel beads. It is worth noting that the residual concentration of H_2O_2 in solution significantly decreased with prolongation of reaction time in the presence of the gel beads, and high Fe content-containing gel beads led to a low residual concentration of H_2O_2 at the same conditions. This confirmed the opinion that the active sites on the gel beads could be Fe containing points that could accelerate the decomposition of H_2O_2 under visible irradiation.

3.3. Photocatalytic activity for dye degradation

3.3.1. Fe content

The degradations of two dyes were conducted at pH 6.0 by the addition of 50 Fe alginate gel beads with different $C_{\text{Fe-bead}}$ to the test solutions under visible light irradiation, and the results are shown in Fig. 8.

Fig. 8 shows that the degradation of the dyes is not found in the presence of only H_2O_2 or the beads. While Fe alginate gel beads were used as the catalysts in the presence of H_2O_2, $D\%$ values of the dyes significantly increased with the prolonging of reaction time, and increasing $C_{\text{Fe-bead}}$ from 0.257 mg to 0.884 mg is accompanied with a remarkable enhancement in the decoloration curve. This indicates that the dye decoloration is faster when Fe alginate gel beads with high Fe content are used as the photocatalysts. This result is similar to our previous observation on the decomposition of azo dye in the system of the Fe amidoximated PAN fiber complex and H_2O_2 [8]. Fernandez et al. [12] found that a significant amount of Fe species was on the surface of the bead and only a smaller fraction inside the cross-linked Fe alginate. Consequently, increasing Fe content caused more active sites on the bead surface, which could decompose H_2O_2 into high concentration of $^\bullet$OH radicals in solution by the heterogeneous photo-Fenton reaction [4], thus promoting the dye degradation. Comparing two dyes, it can be observed that RB 222 has larger $D\%$ values than AB 234 at the same

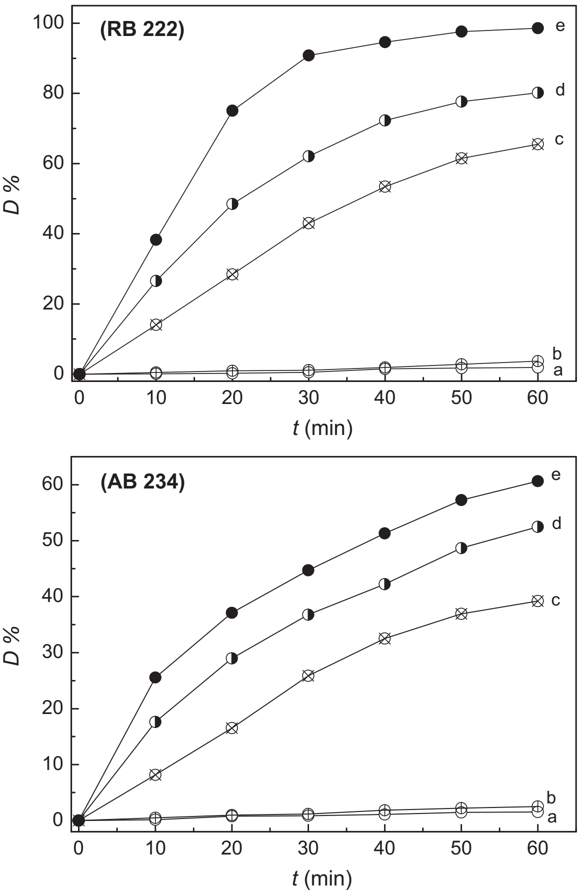

Fig. 8. Degradation profile of azo dyes in different conditions: (a) dye and H_2O_2; (b) dye and beads ($C_{\text{Fe-bead}} = 0.884$ mg); (c) dye, H_2O_2 and beads ($C_{\text{Fe-bead}} = 0.257$ mg); (d) dye, H_2O_2 and beads ($C_{\text{Fe-bead}} = 0.572$ mg); and (e) dye, H_2O_2 and beads ($C_{\text{Fe-bead}} = 0.884$ mg).

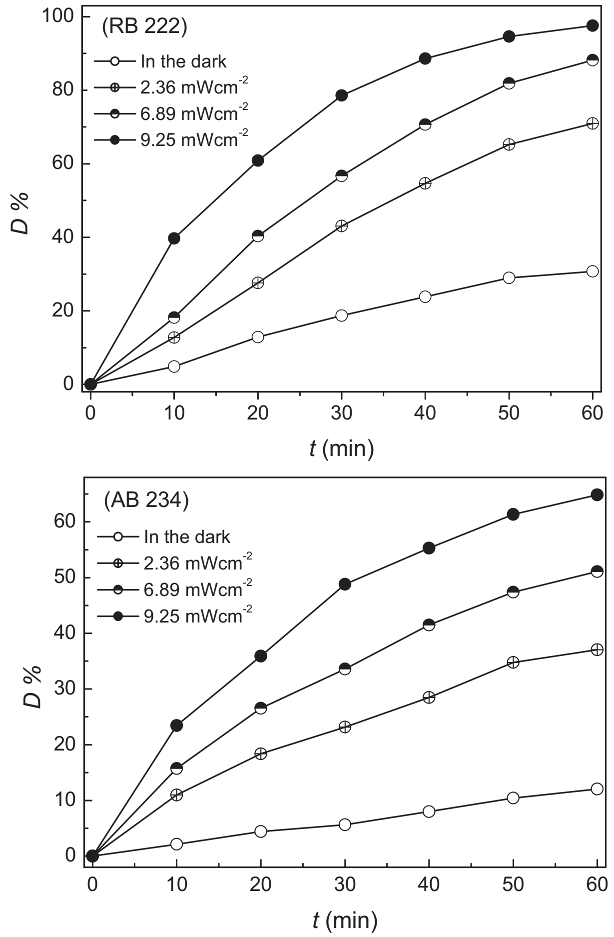

Fig. 9. Relationship between visible irradiation intensity and dye degradation.

$C_{\text{Fe-bead}}$, which is mainly attributed to the differences in molecule structure, particular in numbers of azo units and sulphonate groups between two dyes.

3.3.2. Irradiation intensity

To examine the impact of visible light intensity on the catalytic activity of Fe alginate gel bead, tests were performed at pH 6.0 in dye solutions containing 50 gel beads ($C_{\text{Fe-bead}} = 0.884$ mg) with H_2O_2 induced by different visible light irradiation, as shown in Fig. 9. And a corresponding control experiment in the dark was also examined at the same conditions. It was clearly observed from Fig. 9 that *D*% values gradually increased with irradiation time increasing and decoloration curves varied with light intensity. Moreover, *D*% values in case of light irradiation are much higher than that in the control experiment at the same irradiation time. This means that the dye degradation is slow without light irradiation, and the light irradiation has an enhancing influence on dye degradation in solution. It should be stressed that increasing visible light intensity from 2.36 mW cm^{-2} to 9.25 mW cm^{-2} resulted in a more significant enhancement in *D*% values, suggesting that higher visible light irradiation can improve the catalytic activity of the beads. Therefore, Fe alginate gel beads are considered to be the effective Fenton photocatalysts, which can react with H_2O_2 to generate $^\bullet$OH radicals by the reduction of Fe^{3+} to Fe^{2+} ions on the beads. And the $^\bullet$OH radicals involved were determined by DMPO-trapping ESR technique.

Fig. 10 shows that the signals with intensity of 1:2:2:1 corresponding to the characteristic peak of DMPO–$^\bullet$OH adducts were observed during the degradation process both in the dark and under visible irradiation, and the intensity gradually increased with the prolongation of reaction time. This confirms that the $^\bullet$OH radicals have been formed in the presence of the gel beads during the dye degradation. The resulting $^\bullet$OH radicals can destroy dye molecules into the colorless compounds. A possible reaction pro-

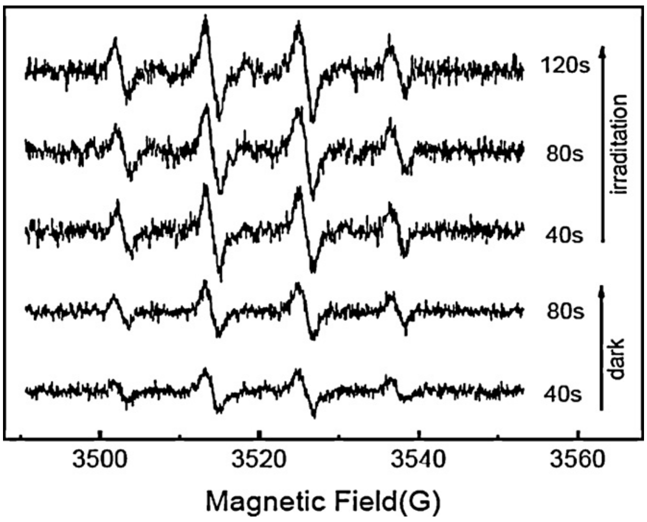

Fig. 10. DMPO spin-trapping ESR spectra recorded at ambient temperature in aqueous solution for DMPO–$^\bullet$OH in RR 222 degradation with H_2O_2 and Fe alginate gel beads ($C_{\text{Fe-bead}} = 0.884$ mg).

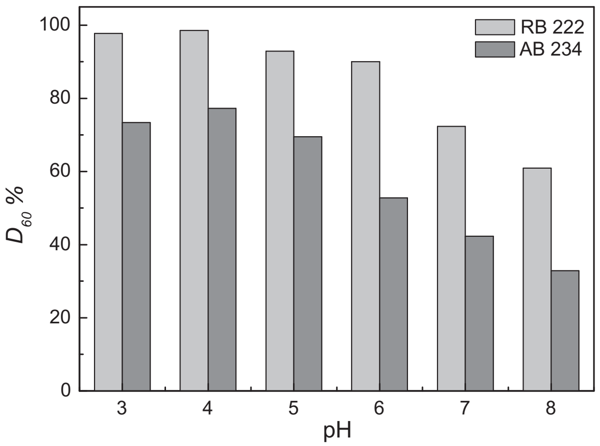

Fig. 11. Degradation of two azo dyes with Fe alginate gel beads in different pH levels.

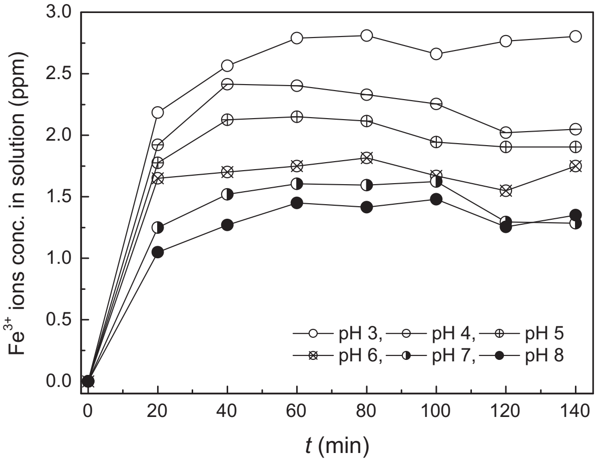

Fig. 12. Effect of pH value on leaching of Fe^{3+} ions from the beads.

cess is expressed by Eqs. (1)–(3):

$$Fe^{3+}/\text{Alginate} + H_2O_2 \xrightarrow{h\nu} Fe^{2+}/\text{Alginate} + HO_2^{\bullet} + H^+ \quad (1)$$

$$Fe^{2+}/\text{Alginate} + H_2O_2 \rightarrow Fe^{3+}/\text{Alginate} + OH^- + HO^{\bullet} \quad (2)$$

$$Fe^{3+}/\text{Alginate} + HO_2^{\bullet} \rightarrow Fe^{2+}/\text{Alginate} + O_2 \quad (3)$$

$$\text{Dye} + Fe^{3+}/\text{Alginate} \xrightarrow{h\nu} \text{Dye}^{*}\text{–}Fe^{3+}/\text{Alginate} \rightarrow \text{Dye}^{\cdot +} + Fe^{2+}/\text{Alginate} \quad (4)$$

$$HO^{\bullet} + \text{Dye}^{\bullet +} \quad \text{or} \quad \text{Dye} \rightarrow \text{Products} \quad (5)$$

Besides, Dhananjeyan et al. [4] reported that an azo dye Orange II was acted as the sensitizer of Fe^{3+}/Nafion/glass fibers to cause a conversion of Fe^{3+} to Fe^{2+} during photoassisted Fenton reaction. In this work, we believed that two azo dyes also have the same effect as Orange II because they have some features in common such as molecular structure and substitutes. Consequently, the photosensitization of the dye molecules adsorbed on the gel beads may lead to a charge transfer with the concomitant quenching of the excited dyes* and the formation of dye^{+}, which is proposed by Eqs. (4) and (5).

3.3.3. *The solution pH*

The catalytic performance of Fe alginate gel beads at different pH values was investigated under visible irradiation in order to ensure their stability as the catalysts at a wide pH range. Fig. 11 shows the decoloration of two dyes with H_2O_2 catalyzed by 50 Fe alginate gel beads ($C_{\text{Fe-bead}} = 0.372$ mg) at a pH 3–8 range within 60 min. It is evident that an efficient breakdown of the dyes has been demonstrated at pH 3 and 4 with highest *D*% values, and *D*% values of two dyes, especially AB 234 deceased as the solution pH value increased. The results primarily indicate that Fe alginate gel beads have excellent catalytic performance at acid pH medium, which is also the optimum pH condition for the heterogeneous photocatalysts such as Fe^{3+}/Nafion membrane [4] as well as iron oxide and silicate nanoparticles [6]. However, *D*% values reached 61.9% for RB 222 and 32.8% for AB 234, respectively at pH 8, suggesting that the beads can provide an acceptable catalytic activity at alkaline condition. This result has an important environmental implication from the viewpoint of low cost and energy saving because acidification is needed to treat many textile effluents, which have an inherent pH value of 7.0–8.0. Moreover, Fenton pretreatment of the dyes is conducted without the need for adjusting subsequently the pH for further less costly biological degradation.

One problem with the heterogeneous photocatalysts is metal leaching from the catalyst that causes secondary contamination to wastewater in pilot-scale application. In order to study the extent of leaching from Fe alginate gel beads, the concentration of Fe^{3+} ions from 50 beads in 200 ml solution was measured by atomic absorption spectrometry method and was shown in Fig. 12.

The results demonstrated that Fe ions were continuously leached out from the beads after the reaction started, and exhibited a wave-like leaching pattern. And the concentration of Fe^{3+} ions in solution declined as pH values increased. The leaching trend is similar to that of the bimetallic Cu/Fe clay catalyst [25]. The final measured concentrations of Fe^{3+} ions in the solution after 140 min were not higher than 3.0 ppm. These results imply that Fe alginate gel beads are used as the effective heterogeneous photocatalysts for the degradation of the azo dye over a broad pH range.

3.3.4. *UV–vis spectrum*

The obvious changes in the photocatalytic decoloration and degradation of two dyes in the presence of Fe alginate gel beads and H_2O_2 under visible illumination using UV–vis absorbance spectra are shown in Fig. 13. And the characteristic absorbance of two dyes is summarized in Table 6.

In general, the absorbance at 400–800 nm corresponds to the n–π^* transition of the azo and hydrazone forms, which is due to the color of azo dyes and it is used to monitor the decoloration. The absorbance at 200–400 nm is attributed to the n–π^* transition of benzene and naphthalene rings, which represent the aromatic content of azo dyes and its decrease is due to the decomposition of aromatic part of the dye [26,27]. It is obvious from Fig. 13 that both the absorbance at 200–400 nm and 400–800 nm of two dyes decrease gradually with prolonging exposure time due to the increase in their decoloration and degradation in water, suggesting that Fe alginate gel beads have the photocatalytic activity for not only the breaking of azo linkages, but also the decomposition of aromatic parts including benzene and naphthalene rings in the dye molecular structure. Moreover, it is observed clearly in Table 6 that the absorption ratios of two dyes at 200–400 nm (290 nm for RB 222, 314 nm for AB 234) are generally higher than those at 400–800 nm (610 nm for RB 222, 452 nm and 601 nm for AB 234) under the same conditions, thus indicating that Fe alginate gel beads show a similar photocatalytic feature to that of Fe-amidoximated PAN fiber complex [8]. This proposes that the aromatic part in the dye molecules, especially those containing more benzene and naphthalene rings such as AB 234 is decomposed with more difficulty than the azo linkages in their molecules.

Table 6
The UV–vis characteristic absorbance of the two dyes.

RB 222			AB 234			
0 min	290 nm 1.00	610 nm 1.00	0 min	314 nm 1.00	452 nm 1.00	601 nm[a] 1.00[b]
30 min	290 nm 0.71	610 nm 0.28	30 min	314 nm 0.84	452 nm 0.53	601 nm 0.39
60 min	290 nm 0.15	610 nm 0.01	60 min	314 nm 0.65	452 nm 0.29	601 nm 0.25

[a] The characteristic absorption wavelengths of the dyes.

[b] The absorption ratios were calculated by A (residual absorption value at the different exposure times)/A_0 (the initial absorption value of the dyes).

3.3.5. TOC measurement

The hydroxyl radical produced from photolysis of Fe alginate gel beads/H_2O_2 system under visible light irradiation may cause mineralization of the dyes, thus producing CO_2 and water. In this work, the mineralization of two dyes was also performed in the presence of Fe alginate gel beads with different $C_{\text{Fe-bead}}$ under light irradiation, and the result is given in Fig. 14.

Fig. 14 shows that TOC removal % of the dyes gradually increased with the prolongation of irradiation time in the aqueous solution. It should be stressed that high $C_{\text{Fe-bead}}$ of the gel beads increases TOC removal % significantly, indicating that the gel beads with high $C_{\text{Fe-bead}}$ as the photocatalysts can lead to a fast mineralization of the dyes at the same light circumference. Additionally, it is apparent that RB 222 is higher than AB 234 in terms of TOC removal % at two $C_{\text{Fe-bead}}$ levels, which implies that the former is mineralized more easily than the latter at the same conditions. These results are well consistent with their decoloration and degradation processes.

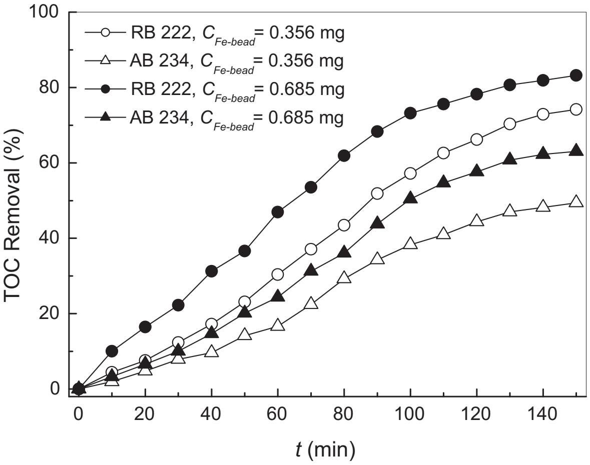

Fig. 14. Mineralization of two dyes in the presence of Fe alginate gel beads with different Fe contents.

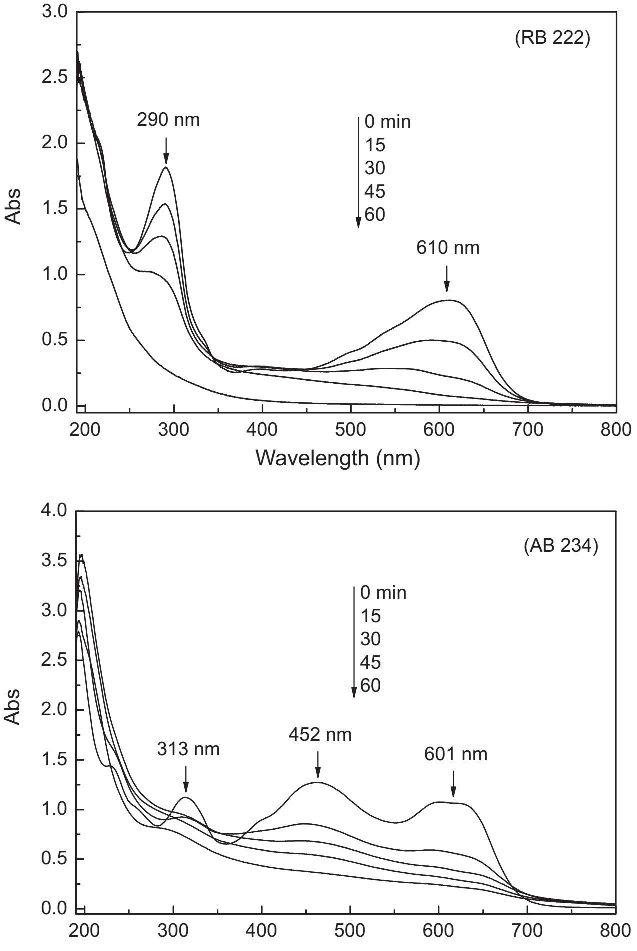

Fig. 13. Changes in UV–vis spectra for degradation of (a) RB 222 and (b) AB 234 in the presence of 50 Fe alginate gel beads ($C_{\text{Fe-bead}}$ = 0.884 mg).

4. Conclusions

Fe alginate gel beads are produced by adding drop-wise sodium alginate solution into $FeCl_3$ gelling solution, and their Fe content increases with the concentration of $FeCl_3$ solution increasing. And Fe^{3+} ion is a central cation that has a coordination number of 6 in the Fe alginate complex. XPS and FT-IR analyses demonstrate that the Fe^{3+} ions reacted with carboxyl groups from glucose chains of alginates through the coordination effect between them to form the Fe alginate gel beads in solution. The Fe containing points on the surface of the gel beads are mainly Fe^{3+} ions, which can accelerate the decomposition of H_2O_2 under irradiation. Fe alginate gel bead can be served as an effective heterogeneous photocatalyst in the degradation of organic dyes in the presence of H_2O_2 in the dark and under visible light irradiation in a wide pH range of 3.0–8.0. And increasing visible irradiation intensity can significantly promote the dye degradation. Moreover, the bead containing high Fe content exhibits a stronger photocatalytic activity towards the oxidative decomposition of the dyes, suggesting that the activity comes from Fe^{3+} ions immobilized on their surface. UV–vis spectra and the TOC measurements indicated that when the beads are used as the photocatalysts, the aromatic parts of the dyes can remarkably be decomposed and mineralized. In summary, Fe alginate gel beads have shown a significant photocatalytic activity for the effective degradation and mineralization of the azo dyes in water under visible light irradiation, and the activity is mainly determined by their Fe content and light irradiation intensity. On the other hand, we have to point out that Fe alginate gel bead is a bit fragile and worn down easily in the reusing process. However, it is possible that the bead can be strengthen by the addition of some metal ions such Ca^{2+} and Cu^{2+} ions during the preparation.

Acknowledgments

This work was kindly supported by a grant from the Natural Science Foundation of China (No. 20773093). The authors thank the support from the Ministry of Education of China through a grant from Research Fund for the Doctoral Program of Higher Education of China (No. 20070058005).

References

[1] E. Forgacs, T. Cserhati, G. Oros, Environ. Int. 30 (2004) 953–971.
[2] J. Fernandez, J. Bandara, A. Lopez, P. Alberz, J. Kiwi, Chem. Commun. (1998) 1493–1494.
[3] J. Fernandez, J. Bandara, A. Lopez, Ph. Buffat, J. Kiwi, Langmuir 15 (1999) 185–192.
[4] M.R. Dhananjeyan, J. Kiwi, P. Albers, O. Enea, Helv. Chem. Acta 84 (2001) 3433–3445.
[5] G.L. Puma, P.L. Yue, Proceedings at the Sixth International Conference on Advanced Oxidation Technologies for Water and Air Remediation, London, Ontario, Canada June 26–30, 2000, pp. 105–106.
[6] J. Feng, X. Hu, P.L. Yue, Ind. Eng. Chem. Res. 42 (2003) 2058–2066.
[7] V.V. Ishtchenko, K.D. Huddersman, R.F. Vitkovskaya, Appl. Catal. A 242 (2003) 123–137.
[8] Y. Dong, Z. Han, C. Liu, F. Du, Sci. Total Environ. 408 (2010) 2245–2253.
[9] A. Martinsen, G. Skjak-Brñk, O. Smidsrd, Biotechnol. Bioeng. 33 (1989) 79–89.
[10] X. Tao, J. Su, L. Wang, J. Chenc, Appl. Catal. A 280 (2008) 186–193.
[11] S. Lim, Y. Zheng, S. Zou, J.P. Chen, Environ. Sci. Technol. 42 (2008) 2551–2556.
[12] J. Fernandez, M.R. Dhananjeyan, J. Kiwi, J. Phys. Chem. B 104 (2000) 5298–5301.
[13] J. Min, J.G. Hering, Water Res. 32 (1998) 1544–1552.
[14] X. Cheng, H. Guan, Y. Su, J. Inorg. Organomet. Polym. 10 (2000) 115–126.
[15] S.K. Papageorgiou, E.P. Kouvelos, E.P. Favvas, A.A. Sapalidis, G.E. Romanos, F.K. Katsaros, Carbohydr. Res. 345 (2010) 469–473.
[16] X.Z. Shu, K.J. Zhu, Eur. J. Pharm. Biopharm. 53 (2002) 193–201.
[17] A. Banerjee, D. Nayak, S. Lahiri, Biochem. Eng. J. 33 (2007) 260–262.
[18] N. Nestle, R. Kimmich, Colloids Surf. A 115 (1996) 147–153.
[19] B. Smith, S. Sridhar, A.A. Khan, Polym. Eur. J. 41 (2005) 1859–1866.
[20] C. Chang, B. Duan, L. Zhang, Polymer 50 (2009) 5467–5473.
[21] C. Prabhu, S. Wanjari, S. Gawande, J. Catal. Mol. B 60 (2009) 13–21.
[22] X. Cheng, H. Guan, Y. Cao, Acta Chim. Sin. 58 (2000) 407–413.
[23] G. Henrici-Oliv, S. Oliv, Coordination Catalysis, Verlag Chemie GmbH, Weinheim, 1977, p. 63.
[24] T. Tripathy, R.P. Singh, J. Appl. Polym. Sci. 81 (2001) 3296–3308.
[25] A.C. Yip, F.L. Lam, X. Hu, Chem. Eng. Sci. 62 (2007) 5150–5153.
[26] H. Park, W. Choi, J. Photochem. Photobiol. A 159 (2003) 241–247.
[27] Y. Dong, J. Chen, C. Li, X. Zhu, Dyes Pigments 73 (2007) 261–268.